The 2015 World Congress on
Advances in Structural Engineering and Mechanics (ASEM15)
Incheon, Korea, August 25-29, 2015

Comparative analyses of conventional prestressed beams and smart prestressed beams

*Weiwei Xu[1)] and Yi Yang[2)]

[1), 2)] *School of Civil Engineering, Southeast University, Nanjing 210096, China*
[1)] xuweiwei@seu.edu.cn

ABSTRACT

Conventional prestressed structures react to all kinds of effects imposed upon them, not accounting for possible excessive stress or continuous deformation during the life of the structures. If some active cables are deployed in a smart prestressed structure, they may be used to prestress the structure online to limit its deflection and stress range due to the various effects. In this paper, a comparative analysis of a conventional prestressed beam and a smart prestressed beam with constraints is investigated. The equations of static equilibrium of the beam under arbitrary loads are presented based on the energy method, and the response of the beam is approximated by the Rayleigh-Ritz method. Furthermore, the response of the beam under moving loads and the service capacity of the beam under uniform load are numerically investigated. The results show that the scope of application of the smart prestressed beam can be much wider than that of the conventional prestressed beam, especially when the beam deflection is strictly limited or the live load is large.

KEYWORDS: active anchorage; smart prestressed beam; deflection control; stress control; service capacity

1. INTRODUCTION

Conventional civil engineering structures are passive structures. Once constructed, the structures are subjected to all types of loading, such as dead load, live load, temperature effect, wind load, seismic load, material property degradation, etc. These loadings on the passive structures could result in excessive stress and continuous deformation. Therefore, the concept of smart structures was seriously considered in the middle of the last century (Yao 1972). Since then, civil engineering structural control methodologies have been rapidly developed and applied over the past several decades (Housner 1997), and an extensive research work has been performed in the field of active structural vibration control (Sheikh 2012).

At the end of the last century, (Montens 1996) and (Sobek 2001) put forward a new concept on active structural shape control under the name of “parastressing” and “adaptive system”. The main purpose of this “smart” prestressing is to bring active

[1)] Associate Professor
[2)] Graduate Student

stiffness in a bridge, and keep the deflection and stress of the bridge within a permissible range when the bridge is subjected to large live load.

In the last decade, several research works have been focused on the smart prestressing. (Deng 2003) have studied the behavior of a concrete specimen uniaxially embedded with a SMA wire actuated by electrical current. (Li 2007)have investigated the behavior of a 20m smart concrete bridge with embedded SMA bundles. (Li 2008) have experimentally studied a simple reinforced concrete beam temporarily strengthened by SMA wires followed by permanent strengthening with CFRP plates. (Xu 2013) have conducted an experimental study on the active shape control of a smart cable-stayed bridge model. However, the static comparative analysis of a conventional prestressed beam (CPB) and a smart prestressed beam (SPB) with constraints is not investigated yet.

In this paper, the equations of static equilibrium of a CPB and a SPB under arbitrary loads are presented based on the energy method, and then the response of the beam is approximated by the Rayleigh-Ritz method. Furthermore, two numerical examples are presented to show the comparative effect of the CPB and the SPB. The results demonstrate that the scope of application of the SPB can be much wider than that of the CPB, especially when the beam deflection is strictly limited or the live load is large.

2. PROBLEM FORMULATION

The SPB always consists of sensors, controllers and actuators communicating via a network, besides the components of the CPB. The beam deflection is measured by the sensor and then transmitted to the controller. After comparing the current deflection with the predefined limit, the controller will send a command to the actuator which can contract or release the prestressed cable, thus changing the beam deflection as a result. Therefore, the beam deflection can be controlled within the permissible range, under various load conditions, if only the beam is collocated with a suitable smart prestressing system.

A simply supported SPB of length l, flexural rigidity EI, with an unbonded prestressed cable of tension rigidity E_sA_s is shown in Fig. 1. The SPB is subjected to an arbitrary distributed load $q(x)$, and a prestressing force T which can be controlled by adjusting the active anchorage length S.

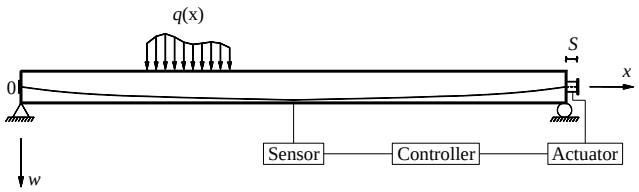

Fig. 1 The SPB under consideration

It is assumed that the rotational inertia, the axial and shear deformation effects of the beam can be neglected and the material is always in the linear-elastic state. The initial state of the SPB is defined as follows: the prestressing force is 0, the arbitrary distributed load is 0, the beam deflection is 0, the prestressed cable shape is $z_0(x)$, and

the active anchorage length is S_0; the final state of the SPB is defined as follows: the prestressing force is T, the arbitrary distributed load is $q(x)$, the beam deflection is $w(x)$, the prestressed cable shape is $z_0(x) + w(x)$, and the active anchorage length is S.

The presented problem is formulated based on the principle of stationary total potential energy. The total potential energy of the system is given by:

$$\Pi = U_1 + U_2 + W_1 + W_2 \tag{1}$$

Where:

- the strain energy of the cable U_1 is:

$$U_1 = \frac{E_s A_s}{2L_0}(\Delta L)^2 \tag{2}$$

- the strain energy of the beam U_2 is:

$$U_2 = \frac{1}{2}\int_0^l EI(w'')^2 dx \tag{3}$$

- the potential energy of the distributed load W_1 is:

$$W_1 = -\int_0^l qw dx \tag{4}$$

- the potential energy of the active anchorage W_2 is:

$$W_2 = -T(S - S_0) \tag{5}$$

The prime denotes differentiation with respect to x. L_0 and ΔL denote the initial length of the cable and the length change of the cable, respectively, expressed as follows:

$$L_0 = \int_0^l \sqrt{1+(z_0')^2}\, dx + S_0 \tag{6}$$

$$\begin{aligned} \Delta L &= \int_0^l \left[\sqrt{1+(z_0'+w')^2} - \sqrt{1+(z_0')^2} \right] dx + S - S_0 \\ &\approx \int_0^l [z_0' w' + \frac{1}{2}(w')^2] dx + S - S_0 \end{aligned} \tag{7}$$

Inserting Eqs. (2-7) into Eq. (1), the total potential energy of the system can be rewritten as follows:

$$\Pi = \frac{E_s A_s}{2L_0}\left\{\int_0^l [z_0' w' + \frac{1}{2}(w')^2]dx + (S - S_0)\right\}^2 + \frac{EI}{2}\int_0^l (w'')^2 dx - \int_0^l qw dx - T(S - S_0) \quad (8)$$

Equating the first variation of the total potential energy to zero, and performing the necessary integration and variation under assumption that the prestressing force *T* has a constant value, leads to

$$\begin{aligned}\delta\Pi &= \frac{E_s A_s \Delta L}{L_0}\left[\int_0^l (z_0'\delta w' + w'\delta w')dx + \delta S\right] + EI\int_0^l w''\delta w'' dx - \int_0^l q\delta w dx - T\delta S \\ &= \int_0^l \left\{EIw'''' - \frac{E_s A_s \Delta L}{L_0}(z_0'' + w'') - q\right\}\delta w dx + \\ &\quad \left\{\frac{E_s A_s \Delta L}{L_0}(z_0' + w') - EIw'''\right\}\delta w\Big|_0^l + EIw''\delta w'\Big|_0^l + \left(\frac{E_s A_s \Delta L}{L_0} - T\right)\delta S \\ &= 0\end{aligned} \quad (9)$$

Knowing that virtual displacements *δw*, *δw'* and *δS* are arbitrary, the following governing equations can be obtained:

$$EIw'''' - \frac{E_s A_s \Delta L}{L_0}(z_0'' + w'') - q = 0 \quad (10)$$

$$\frac{E_s A_s \Delta L}{L_0} - T = 0 \quad (11)$$

Inserting Eqs. (6-7) into Eq. (10), the governing equation of the SPB can be obtained:

$$EIw'''' - E_s A_s \frac{\int_0^l \left[z_0' w' + \frac{1}{2}(w')^2\right]dx + (S - S_0)}{\int_0^l \left[1 + \frac{1}{2}(z_0')^2\right]dx + S_0}(z_0'' + w'') - q = 0 \quad (12)$$

Inserting Eqs. (6-7) into Eq. (11), the prestressing force *T* can be obtained:

$$T = E_s A_s \frac{\int_0^l \left[z_0' w' + \frac{1}{2}(w')^2\right]dx + (S - S_0)}{\int_0^l \left[1 + \frac{1}{2}(z_0')^2\right]dx + S_0} \quad (13)$$

The maximum and minimum stress at the mid-span section of the beam can be expressed:

$$\sigma = \frac{N}{A} \pm \frac{M}{W} \tag{14}$$

Where:

- the axial force at the centroid of the section *N* is:

$$N = T \tag{15}$$

- the moment at the centroid of the section *M* is:

$$M = \frac{\int_0^l q(l-x)dx}{2} - \int_0^{l/2} q(\frac{l}{2}-x)dx - Tz_0(\frac{l}{2}) \tag{16}$$

A and *W* denote the area and the cross section factor, respectively.

Additionally, when *S* is a constant S_c (greater than S_0) in Eq. (12), the governing equation of a CPB can be obtained:

$$EIw'''' - E_s A_s \frac{\int_0^l \left[z_0' w' + \frac{1}{2}(w')^2 \right] dx + (S_c - S_0)}{\int_0^l \left[1 + \frac{1}{2}(z_0')^2 \right] dx + S_0} (z_0'' + w'') - q = 0 \tag{17}$$

When $E_s A_s$ is equal to zero in Eq. (12), the governing equation of a beam without prestressing can be obtained:

$$EIw'''' - q = 0 \tag{18}$$

It can be found from Eq. (12) that, for a certain SPB, the beam deflection *w* is determined by the distributed load *q* and the active anchorage length *S*. In other words, the beam deflection can be controlled within a permissible range under some load conditions, by means of adjusting the active anchorage length.

Assuming the control object is to keep the mid-span deflection *f* within the permissible deflection limits ($\delta_1 \le f \le \delta_2$), the response of the SPB given by Eq. (12) can be approximated by the Rayleigh-Ritz method as follows:

- the deflection equation of the beam *w* is:

$$w = \sum_{n=1}^{\infty} a_n \sin \frac{n\pi x}{l} \tag{19}$$

- the cable shape z_0 is:

$$z_0 = \sum_{n=1}^{\infty} b_n \sin\frac{n\pi x}{l} \tag{20}$$

- the uniform load p is rewritten as:

$$q = \frac{4p}{\pi} \sum_{n=1,3,5}^{\infty} \frac{1}{n} \sin\frac{n\pi x}{l} \tag{21}$$

- the concentrated load P at the point (k, 0) is rewritten as:

$$q = \frac{2P}{l} \sum_{n=1}^{\infty} \sin\frac{n\pi k}{l} \sin\frac{n\pi x}{l} \tag{22}$$

Substituting Eqs. (19-22) into Eq. (12), the governing equation of the SPB takes the form:

$$EI\sum_{n=1}^{\infty} a_n \left(\frac{n\pi}{l}\right)^4 \sin\frac{n\pi x}{l} + E_s A_s \frac{\pi^2(2\sum_{n=1}^{\infty} a_n b_n n^2 + \sum_{n=1}^{\infty} a_n^2 n^2) + 4l(S - S_0)}{\pi^2 \sum_{n=1}^{\infty} b_n^2 n^2 + 4l(l + S_0)} \sum_{n=1}^{\infty} (a_n + b_n)\left(\frac{n\pi}{l}\right)^2 \sin\frac{n\pi x}{l} = \frac{4p}{\pi} \sum_{n=1,3,5}^{\infty} \frac{1}{n} \sin\frac{n\pi x}{l} + \frac{2P}{l} \sum_{n=1}^{\infty} \sin\frac{n\pi k}{l} \sin\frac{n\pi x}{l} \tag{23}$$

Expressing Eq. (23) in sine series and setting the coefficients to zero, we can obtain n equations with n+1 unknowns (a_1 , a_2 ,…, a_n and S). Considering the mid-span deflection constraint equation, the solution can be easily implemented in Matlab, and the recurrence relation from the ith load step to the (i+1)th load step is given as follows:

(a) Let $S = S_i$, then $a_1, a_2, \ldots, a_n$ can be obtained by substituting S into Eq. (23), and $f_i = \sum_{n=1,3,5}^{\infty} a_n$

(b) If $\delta_1 \le f_i \le \delta_2$, then $S_{i+1} = S_i$, and $f_{i+1} = f_i$. If $f_i > \delta_2$, then S_{i+1} can be obtained by substituting $\sum_{n=1,3,5}^{\infty} a_n = \delta_2$ into Eq. (23), and $f_{i+1} = \delta_2$. If $f_i < \delta_1$, then S_{i+1} can be obtained by substituting $\sum_{n=1,3,5}^{\infty} a_n = \delta_1$ into Eq. (23), and $f_{i+1} = \delta_1$.

The mid-span deflection of the beam and the length change of the anchorage, under different load conditions, can be obtained by using the above recurrence relation and setting the initial value i = 0. At the same time, the maximum and minimum stress at the mid-span section of the beam can be solved using Eqs. (13-16).

The control object can also be to keep the extreme stress σ within the permissible stress limits ($\sigma_1 \le \sigma \le \sigma_2$), and the response of the SPB can be approximated by the similar method described above.

3. NUMERICAL ANALYSIS

In this section, two examples are presented to illustrate the comparative effect of the CPB and the SPB. In the first example, the response of a simply supported beam under moving loads is investigated. In the second example, the service capacity of the beam under uniform load is investigated. All of the numerical calculations in this section were carried out in Matlab.

The beam under study is 25 m long and 3.7 m wide, as shown in Fig. 2. The beam is designed as CPB and SPB respectively, and is modeled as an Euler-Bernoulli beam with equal stiffness.

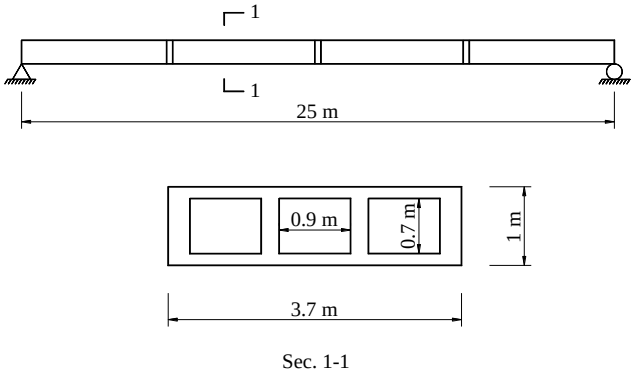

Fig. 2 Elevation and cross section of the beam

The beam mass density ρ = 2840 kg/m^3, concrete Young's modulus E = 25907 MPa, and concrete compressive strength f_c = 30 MPa. The beam length l = 25 m, girder cross-sectional area A = 1.81 m^2, moment of inertia I = 0.2311 m^4, and dead load p = 50.376 kN/m. In addition, the post-tensioned steel cables' modulus of elasticity E_s = 200 GPa, and the cables cross-sectional area A_s = 0.01251 m^2. When the beam is subjected to no load, the cable shape $z_0(x) = 0.45\sin(\pi x/25)$ and the anchorage length S_0 = 0.4 m.

3.1 Moving load

In this example, the response of the beam under different moving loads is investigated. The purpose of the active anchorage in the SPB is to keep the beam deflection in the range of -0.005 to 0.02 m.

The initial state, for both the CPB and the SPB, is that the midspan deflection is zero when the beam is only subjected to its own weight. Then, the initial length of the anchorage is equal to 0.4917 m.

Assuming the concrete beam will not be cracked or vibrated, the midspan deflection and the anchorage length of the CPB along with the variation of the moving load

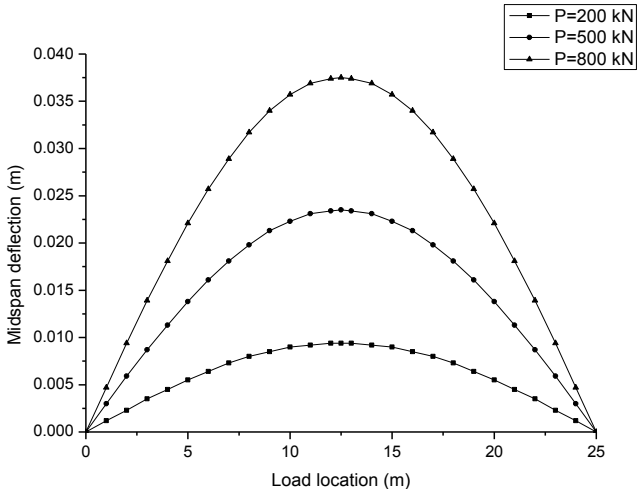

Fig. 3 The CPB deflection response to the changes in the load

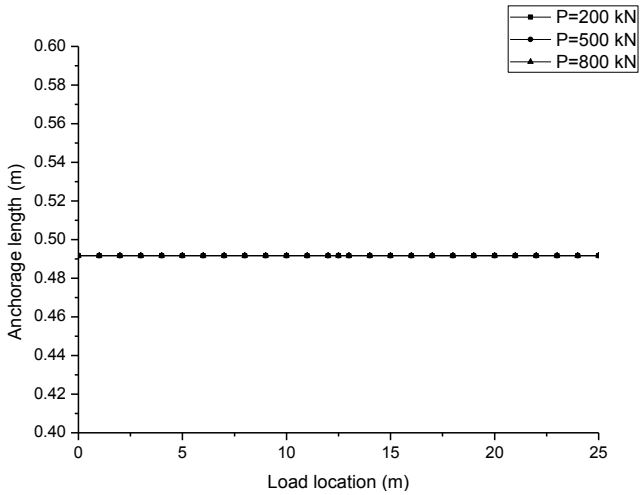

Fig. 4 The CPB anchorage response to the changes in the load

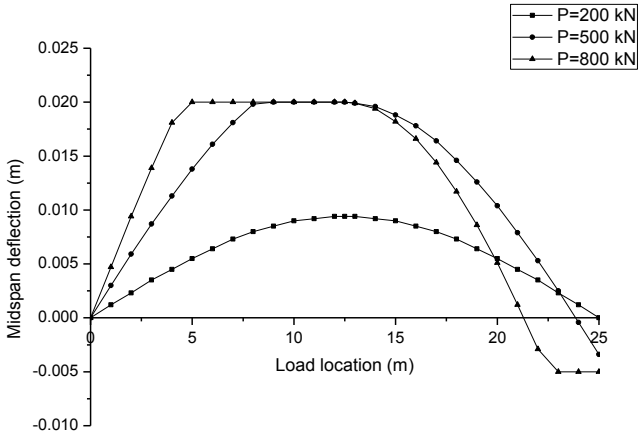

Fig. 5 The SPB deflection response to the changes in the load

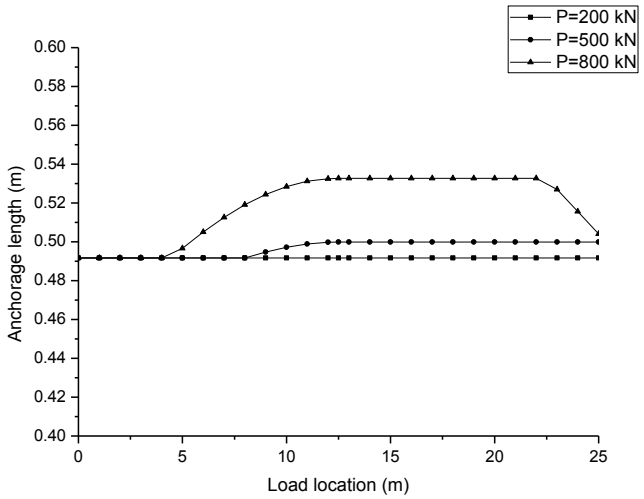

Fig. 6 The SPB anchorage response to the changes in the load

location are shown in Figs. 3 and 4, respectively. The results of the SPB are shown in Figs. 5 and 6.

Fig. 3 shows that the midspan deflections of the CPB only under the light moving load can be in the predefined range. The anchorage lengths of the CPB are all equal to its initial length, as shown in Fig. 4. Comparing with Fig. 3, Fig. 5 shows that the midspan deflections of the SPB under the light, moderate and heavy loads are all kept in the predefined range. Furthermore, the anchorage length is not necessary to be changed under the light load condition; the anchorage length under the moderate load condition needs to be increased as the midspan deflection reaches the positive limit, and needs not to be decreased; the anchorage length under the heavy load condition needs to be increased as the midspan deflection reaches the positive limit, and needs to be decreased as the midspan deflection reaches the negative limit, as shown in Fig. 6.

Comparing Fig. 5 with Fig. 3, it can be seen that the SPB might not be restored to its initial state as the load leaves the beam. When the loads move through the SPB successively, the midspan deflection and the anchorage length along with the variation of the moving conditions are shown in Figs. 7 and 8, respectively.

Fig. 7 shows that the midspan deflections under the four conditions are all kept in the predefined range. Comparing Fig. 8(d) with Fig. 8(b), the anchorage length under the load condition of 537 kN needs not to be changed, however, the anchorage length under the load condition of 500 kN needs to be increased. It can be concluded that whenever the deflection under a moving load reaches the positive limit, the maximum load, under which condition the anchorage length just needs not to be changed, is increased until the deflection reaches the negative limit. In another word, the SPB has a certain adaptive ability under several heavy load conditions.

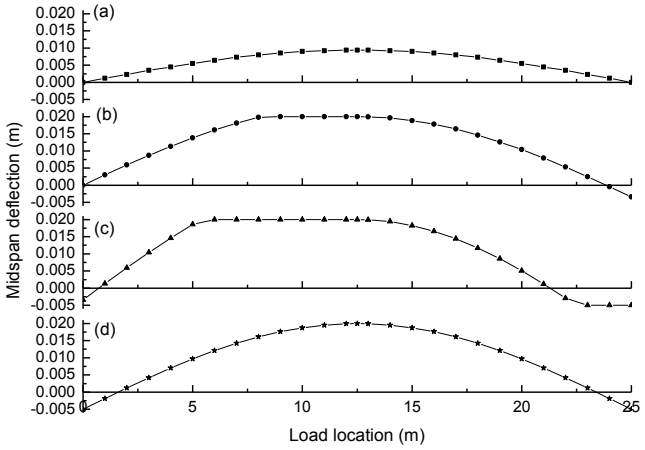

Fig. 7 The SPB deflection response to the successive changes in the load: (a) P = 200 kN, (b) P = 500 kN, (c) P = 800 kN, (d) P = 537 kN

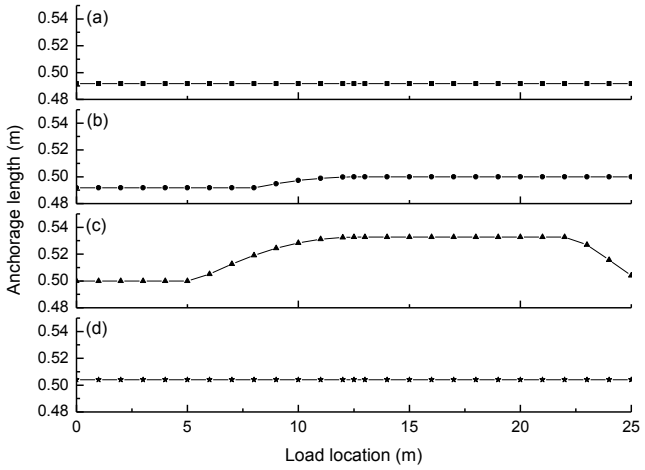

Fig. 8 The SPB anchorage response to the successive changes in the load: (a) P = 200 kN, (b) P = 500 kN, (c) P = 800 kN, (d) P = 537 kN

Furthermore, Figs. 7(d) and 8(d) show that the 537 kN load is a critical load of the SPB. When the subsequent moving load is less than 537 kN, the anchorage length needs not to be changed. Otherwise, the anchorage length needs to be both increased and decreased.

3.2 Uniform load

In this example, the service capacity of the beam under uniform load is investigated. The cables in the beam serve the purpose of controlling both cracking and deflection.

The following constraints [10] are taken into account: (a) The concrete stress should not exceed the allowable tensile stress σ_1 = -2.7386 MPa, or allowable compressive stress σ_2 =13.5 Mpa. (b) The beam deflection under live load should not exceed 0.025 m, which is 1/1000 of the span length. (c) The cable stress should not exceed 1395

MPa, which is 75% of the characteristic tensile strength of prestressing steel. (d) The maximum length of the anchorage can reach 0.6 m. (e) The minimum live load is zero.

Firstly, the service capacity of the CPB under uniform load is investigated, as shown in Fig. 9.

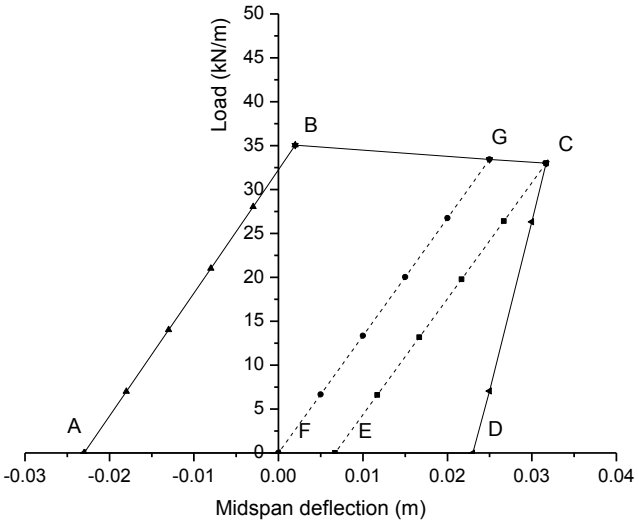

Fig. 9 The service capacity of the CPB

The region ABCDA shows the feasible region of the live load versus the midspan deflection curves of the CPB. The point A corresponds to the maximum permissible camber of the beam under dead load, as the concrete on the bottom surface reaches the allowable compressive stress. The line AB is the live load versus the midspan deflection curve of the maximum camber beam. The line BC corresponds to the beam deflection limit. The line CD corresponds to the limit state in which the concrete on the bottom surface reaches the allowable tensile stress. The line DA corresponds to the minimum live load limit. Comparing with the point A, the point D corresponds to the maximum permissible deflection of the beam under dead load, as the concrete on the bottom surface reaches the allowable tensile stress.

From the point D to A along the line DA, the corresponding initial prestressing force of the CPB is increasing. Besides the line AB, there exist another two special curves, as dashed lines shown in Fig. 9. The dashed line FG is the live load versus the midspan deflection curve of the beam whose initial state is the beam has no deflection under dead load. The dashed line EC is the live load versus the midspan deflection curve of the beam whose final state is the beam reaches the deflection limit, as well as the concrete on the bottom surface reaches the allowable tensile stress. Comparing the lines AB with FG and EC, it can be concluded that the stiffness of the CPB has a very slight positive correlation with the initial prestressing force. Consequently, the live load versus the midspan deflection curve of the beam whose initial state is corresponded to the point in the line AE will reach the beam deflection limit, but the curve from the other initial state will reach the allowable tensile stress of the concrete.

Secondly, the service capacity of the SPB under uniform load is investigated, as shown in Fig. 10.

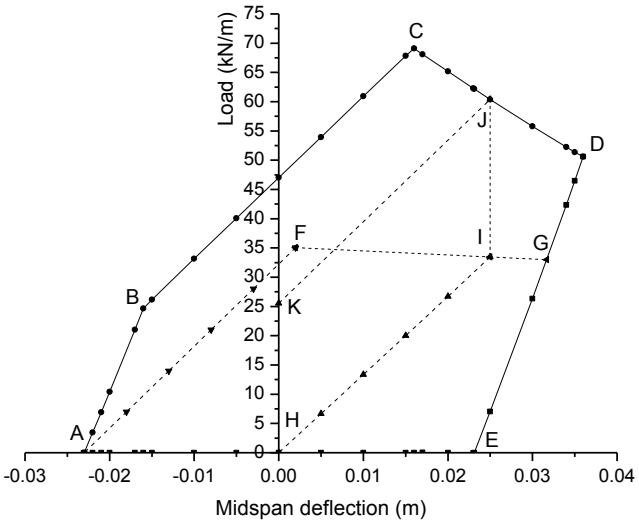

Fig. 10 The service capacity of the SPB

The region ABCDEA shows the feasible region of the live load versus the midspan deflection curves of the SPB. The line AB corresponds to the limit state in which the concrete on the bottom surface reaches the allowable compressive stress. The line BC corresponds to the limit state in which the cable stress reaches its allowable tensile stress. The line CD corresponds to the limit state in which the concrete on the top surface reaches the allowable compressive stress. The line DE corresponds to the limit state in which the concrete on the bottom surface reaches the allowable tensile stress. The line EA corresponds to the minimum live load limit. Obviously, the region AFGEA for the CPB is included in the region ABCDEA.

The live load of the SPB can reach more higher than that of the CPB. For instance, to the beam whose initial state is the beam has no deflection under dead load, the maximum live load of the CPB can reach the point I along the dashed line HI, however, the live load of the SPB can continue to reach the point J along the dashed line IJ. Furthermore, the live load of the CPB will decrease only from the point I to H along the dashed line IH, but the live load of the SPB can decrease from the point J to I and then H along the dashed lines JI and IH, or from the point J to K and then H along the dashed lines JK and KH, or from the point J to any other point satisfying the constrains and then to H. Comparing with a certain stiffness of the CPB, the stiffness of the SPB can be arbitrarily chosen, as long as the beam satisfies the constraints.

Fig. 10 also indicates that the maximum live load of the SPB is approximately twice of that of the CPB. That ratio will be higher for smaller deflection limit. It follows that the scope of application of the SPB can be much wider than the CPB, especially when the beam deflection is strictly limited or the live load is large.

4. CONCLUSIONS

This paper presents a comparative analysis of a CPB and a SPB with constraints. The equations of static equilibrium of the beam under arbitrary loads are presented

based on the energy method, and the response of the beam is approximated by the Rayleigh-Ritz method. Furthermore, the response of the beam under moving loads and the service capacity of the beam under uniform load are numerically investigated. The results show that the scope of application of the SPB can be much wider than that of the CPB, especially when the beam deflection is strictly limited or the live load is large.

The SPB also has some other advantages over the CPB: the beam can be designed more lightly with the same constrains; the permanent undesirable stresses can be avoided; the level of creep damage can be significantly decreased; the prestressing losses can be easily compensated. However, there still remain many unanswered questions that need further study. For example, powerful actuator systems and stable sensor systems for long-term applications should be developed, as well as the economics of the SPB over the full life cycle need to be analyzed.

ACKNOWLEDGMENTS

This work is supported by the National Natural Science Foundation of China (No. 51208094), the Natural Science Foundation of Jiangsu Province (No. BK2012342), and the Priority Academic Program Development of Jiangsu Higher Education Institutions (No. CE01-3-05).

REFERENCES

Zongcai Deng, Qingbing Li, Anquan Jiu and Lei Li (2003) Behavior of concrete driven by uniaxially embedded shape memory alloy actuators. Journal of Engineering Mechanics 129(6):697-703

Housner, G. W., et al. (1997) Structural control: past, present, and future. Journal of Engineering Mechanics 123(9):897-971

Hui Li, Zhi-qiang Liu and Jin-ping Ou (2008) Experimental study of a simple reinforced concrete beam temporarily strengthened by SMA wires followed by permanent strengthening with CFRP plates. Engineering Structures 30(3):716-723

Lei Li, Qingbin Li and Fan Zhang (2007) Behavior of smart concrete beams with embedded shape memory alloy bundles. Journal of Intelligent Material Systems and Structures 18(10):1003-1014

Montens, S. (1996) A Global Concept for 21st Century Bridges: Parastressing. Proc., FIP Symposium on Post-tensioned Concrete Structures, London, UK, September

Sheikh, M. N., Xiong, J. and Li, W. H. (2012) Reduction of seismic pounding effects of base-isolated RC highway bridges using MR damper. Structural Engineering and Mechanics 41(6):791-803

Sobek W. and Teuffel P. (2001) Adaptive systems in architecture and structural engineering. Proceedings of SPIE, Newport Beach, USA, July

Weiwei Xu, Masri, S. F., Zhitao Lv, and Hanshan Ding (2013) An experimental study on the active shape control of a smart cable-stayed bridge model. Structural Control and Health Monitoring 20(7):1096-1105

Yao, J. T. P. (1972) Concept of structural control. Journal of Structural Division 98(7):1567-1574
AASHTO (2004) AASHTO LRFD bridge design specifications, SI Units. 3rd ed. Washington DC, USA